REGULAR ARTICLE

blood advances

Nix-mediated mitophagy regulates platelet activation and life span

Weilin Zhang,[1] Qi Ma,[2,3] Sami Siraj,[1,4] Paul A. Ney,[5,6] Junling Liu,[7] Xudong Liao,[8,9] Yefeng Yuan,[10-12] Wei Li,[10-12] Lei Liu,[1] and Quan Chen[1,13]

[1]State Key Laboratory of Membrane Biology, Institute of Zoology, Chinese Academy of Sciences, Beijing, China; [2]State Key Laboratory of Membrane Biology and [3]Beijing Key Laboratory of Cardiometabolic Molecular Medicine, Peking-Tsinghua Center for Life Sciences, Institute of Molecular Medicine, Peking University, Beijing, China; [4]Institute of Basic Medical Sciences, Khyber Medical University, Peshawar, Pakistan; [5]Department of Cell and Molecular Biology and [6]Lindsley Kimball Research Institute, New York Blood Center, New York, NY; [7]Department of Biochemistry and Molecular Cell Biology, Shanghai Key Laboratory of Tumor Microenvironment and Inflammation, Shanghai Jiaotong University, Shanghai, China; [8]Case Cardiovascular Research Institute, School of Medicine, Case Western Reserve University, Cleveland, OH; [9]Harrington Heart and Vascular Institute, University Hospitals Cleveland Medical Center, Cleveland, OH; [10]Beijing Key Laboratory for Genetics of Birth Defects and [11]MOE Key Laboratory of Major Diseases in Children, Center for Medical Genetics, Beijing Pediatric Research Institute, Beijing Children's Hospital/Capital Medical University/National Center for Children's Health, Beijing, China; [12]Shunyi Women and Children's Hospital of Beijing Children's Hospital, Beijing, China; and [13]Tianjin Key Laboratory of Protein Science, College of Life Sciences, Nankai University, Tianjin, China

Key Points

- Nix controls platelet activation/arterial thrombosis, regulating platelet mitochondria quality/activity in (patho)physiological settings.
- Knockout of *Nix* increases the life span of platelets by inhibiting autophagic degradation of the mitochondrial protein Bcl-xL.

Platelet activation requires fully functional mitochondria, which provide a vital energy source and control the life span of platelets. Previous reports have shown that both general autophagy and selective mitophagy are critical for platelet function. However, the underlying mechanisms remain incompletely understood. Here, we show that Nix, a previously characterized mitophagy receptor that plays a role in red blood cell maturation, also mediates mitophagy in platelets. Genetic ablation of *Nix* impairs mitochondrial quality, platelet activation, and $FeCl_3$-induced carotid arterial thrombosis without affecting the expression of platelet glycoproteins (GPs) such as GPIb, GPVI, and $\alpha_{IIb}\beta_3$. Metabolic analysis revealed decreased mitochondrial membrane potential, enhanced mitochondrial reactive oxygen species level, diminished oxygen consumption rate, and compromised adenosine triphosphate production in $Nix^{-/-}$ platelets. Transplantation of wild-type (WT) bone marrow cells or transfusion of WT platelets into Nix-deficient mice rescued defects in platelet function and thrombosis, suggesting a platelet-autonomous role (acting on platelets, but not other cells) of Nix in platelet activation. Interestingly, loss of *Nix* increases the life span of platelets in vivo, likely through preventing autophagic degradation of the mitochondrial protein Bcl-xL. Collectively, our findings reveal a novel mechanistic link between Nix-mediated mitophagy, platelet life span, and platelet physiopathology. Our work suggests that targeting platelet mitophagy Nix might provide new antithrombotic strategies.

Introduction

Circulating platelets are anucleated blood cells that play key roles in thrombosis and hemostasis.[1-4] Upon vascular injury or under conditions of high shear stress, platelets can be activated by their interaction with von Willebrand factor and collagen, or by various soluble agonists, such as thrombin, adenosine 5′-diphosphate (ADP), and thromboxane A_2. These factors simultaneously activate a signaling network via their respective receptors, which include glycoprotein Ib (GPIb), GPVI, protease-activated receptors, and $P2Y_{12}$.[1,2] Subsequently, the platelet signaling pathways converge to trigger multiple responses in platelets, such as shape change, secretion of granules, and "inside-out" signaling pathways leading to activation of integrin $\alpha_{IIb}\beta_3$. Ligand binding to integrin $\alpha_{IIb}\beta_3$ mediates platelet adhesion and platelet aggregation and induces "outside-in" signaling pathways, which further results in more platelet spreading, granule secretion, platelet adhesion and aggregation, physiological clot retraction, or pathological thrombus formation.[1,2]

Submitted 26 January 2019; accepted 14 May 2019. DOI 10.1182/bloodadvances.2019032334.

The full-text version of this article contains a data supplement.

Platelet activation is highly energy-dependent and heavily relies on fully functional mitochondria, although only small numbers of fully functional mitochondria are contained in a single platelet.[5,6] Interestingly, mitochondria control the life span of platelets through a mechanism involving a mitochondrial protein, Bcl-xL.[7,8] Specifically, Bcl-xL, the master regulator of mitochondrial apoptosis and mitochondrial physiology, interacts with the proapoptotic Bcl-2–family protein Bak to determine the life span of platelets.[7,8] It has been confirmed that the level of Bcl-xL that platelets inherited from megakaryocytes sets platelet life span. Inactivation of Bcl-xL by pharmacological inhibition or genetic ablation decreases platelet half-life and incurs platelet apoptosis and thrombocytopenia.[7,8] Therefore, mitochondria are essential for the proper functions and life span of platelets.[6] Conversely, impaired mitochondrial dysfunction with abnormal respiratory chain electron transfer and adenosine triphosphate (ATP) energy generation in platelets causes reduced ATP production, impaired calcium buffering, generation of mitochondrial reactive oxygen species (ROS), and even programmed cell death, and has been linked with the occurrence of diabetes and cardiovascular diseases.[6,9,10]

Mitochondrial homeostasis is tightly regulated to ensure optimal mitochondrial number and appropriate quality to sustain physiological functions.[6,10,11] For example, mitochondria undergo constant fission/fusion cycles, which provide a mechanism to repair or dilute defects in mitochondria.[11,12] Severely damaged mitochondria beyond repair are segregated from the mitochondrial network by mitochondrial fission and are eliminated through mitochondrial autophagy (removal of mitochondria) or apoptosis (removal of cells).[13] Mitochondrial autophagy, also called mitophagy, is a selective process that delivers damaged mitochondria into autophagosomes for lysosomal degradation.[14-24] Currently, Parkin/PINK1 (phosphatase and tensin homolog-induced putative kinase 1)–mediated mitophagy and receptor-mediated mitophagy are considered 2 major mitophagy pathways in yeast and mammalian cells.[25-28] Specifically, upon the loss of mitochondrial membrane potential, PINK1 becomes stabilized and accumulates on the outer mitochondrial membrane, resulting in phosphorylation of ubiquitin and Parkin and the recruitment of autophagy receptors. The phosphorylated Parkin is activated to mediate ubiquitination of various outer mitochondrial membrane proteins, leading to mitochondrial fission and autophagic degradation of damaged mitochondria.[29]

We have shown that FUN14 domain-containing 1 (FUNDC1) mediates hypoxia-induced mitophagy by its direct interaction with microtubule-associated proteins 1A/1B light chain 3A (LC3) through the conserved LC3-interacting region (LIR).[6,30,31] Furthermore, FUNDC1-mediated mitophagy in response to hypoxia in platelets plays a critical role in platelet activation.[6] Nix (also known as BNIP3L), a B-cell lymphoma 2 (BCL2)–interacting protein that localizes to endoplasmic reticulum and mitochondria, also harbors a LIR to interact with LC3 and plays an important role in the clearance of mitochondria by mitophagy during the maturation of reticulocytes.[14,32-35] Loss of *Nix* leads to mitochondrial retention in erythrocytes, defective erythroid maturation, and anemia.[14,32,33,36-38] Because both platelets and red blood cells are anucleates from the same hematopoietic cell lineage,[39] we were interested to investigate whether Nix plays a role in mediating mitophagy in platelets. We discovered that Nix indeed mediates mitophagy in platelets, which is critical for mitochondrial quality control, platelet activation, and thrombosis. Loss of *Nix* also increased the life span of platelets in vivo by inhibiting autophagic degradation of the mitochondrial protein Bcl-xL.

Materials and methods

Reagents

Thrombin was purchased from the Enzyme Research Laboratories. Bovine serum albumin (BSA) and dimethyl sulfoxide (DMSO) were purchased from Sigma. Fluorescein isothiocyanate (FITC)-conjugated goat anti-mouse (GAM) immunoglobulin G (IgG), FITC-conjugated goat anti-rabbit IgG, GAM immunoglobulin conjugated with horseradish peroxidase and goat anti-rabbit immunoglobulin conjugated with horseradish peroxidase were purchased from DAKO. Antibodies included anti-Tom20 (1:1000; Abcam), anti-LC3 polyclonal antibody (1:1000; BD Biosciences), anti-Tim23 (1:1000; BD Biosciences), anti-P62 (1:1000; BD Biosciences), and anti–the active $\alpha_{IIb}\beta_3$ antibody (clone/isotype: JON/A/Rat; Wistar) IgG2b. The antibody of phycoerythrin-conjugated JON/A specifically binds to the active form of mouse integrin $\alpha_{IIb}\beta_3$,[18] and anti-actin (1:1000; Sigma) was used in this study. Anti-FUNDC1 (1:1000) polyclonal antibody was produced in our laboratory as described previously.[6] All other antibodies were purchased from Cell Signaling Technology (Danvers, MA) and all reagents were from Sigma Aldrich, unless otherwise noted. All of the experiments involving carbonyl cyanide-*p*-trifluoromethoxyphenylhydrazone (FCCP) are ex vivo treatment of platelets.

Mice

Nix$^{-/-}$ mice were generated as described previously.[36] *Nix*$^{-/-}$ mice were backcrossed to C57BL/6 mice for at least 6 generations. *Nix*$^{-/-}$ mice and their controls were maintained and bred in the Center for Experimental Animals at the Institute of Zoology, Chinese Academy of Sciences, Beijing, China. All mouse studies were approved by the animal care and use committee of the Institute of Zoology, Chinese Academy of Sciences, Beijing, China, and the studies conformed to the directions for the care and use of laboratory animals.

Platelet preparation

Washed platelets were prepared as described previously.[6] The method was approved by the institutional review board of the Institute of Zoology, Chinese Academy of Sciences, Beijing, China. Briefly, the *Nix*$^{-/-}$ mice (8 weeks old) and their controls were anesthetized with pentobarbital (70 mg/kg, intraperitoneally). Whole blood from *Nix* knockout mice or wild-type (WT) mice was harvested from the abdominal aorta using a one-seventh volume of acid-citrate-phosphate (2% dextrose, 1.5% citric acid, and 2.5% trisodium citrate containing 1 U/mL apyrase) as anticoagulant. To prepare washed platelets, whole blood in acid-citrate-phosphate containing 1 U/mL apyrase was centrifuged at 180*g* for 10 minutes to obtain platelet-rich plasma. After washing twice with 0.0129 M trisodium citrate, 0.03 M D-glucose, 0.12 M sodium chloride (pH 6.5), the obtained platelet pellets were resuspended in modified Tyrode buffer (MTB) (2 mM KCl, 0.34 mM Na_2HPO_4, 0.35% bovine serum albumin, 12 mM $NaHCO_3$, 1 mM $MgCl_2$, 5 mM *N*-2-hydroxyethylpiperazine-*N*′-2-ethanesulfonic acid [HEPES], 137 mM NaCl, and 5.5 mM glucose).

Platelet aggregation

For the studies of platelet aggregation in vitro, the washed *Nix*$^{-/-}$ and control platelets (3×10^8/mL) were first pretreated with

FCCP (5 μM) or vehicle control DMSO at room temperature for 120 minutes or at the indicated time, and then the treated platelets were incubated with α-thrombin (0.05 U/mL), collagen (0.5 μg/mL), ADP (10 μM), or a thromboxane A2 analog, U46619 (350 nM). Platelet aggregations were finally conducted and analyzed using a turbidometric aggregometer (Precil LBY-NJ; Xinpusen) at a stirring speed of 1000 rpm at 37°C.

Western blots

The washed *Nix*$^{-/-}$ and control platelets (3 × 10^8/mL) were pretreated with FCCP (5 μM) or vehicle control DMSO at room temperature for 120 minutes or at the indicated time, and then resuspended in MTB and lysed in 2× platelet lysis buffer including 2% Triton X-100, 0.01 M EGTA, 0.1 M Tris, 0.15 M NaCl, 1 mM dithiothreitol, phenylmethylsulfonyl fluoride (1 mM), E64 (0.1 mM), and 1/100 aprotinin at a volume ratio of 1:1 for 30 minutes. The prepared platelet samples were analyzed by sodium dodecyl sulfate polyacrylamide gel electrophoresis and western blotting using the indicated antibodies (anti-LC3, anti-P62, anti-Tom20, anti-Tim23, anti-Nix, anti-actin, etc). All immunoblot data except those in supplemental Figure 9 are total platelet lysates.

Coimmunoprecipitation between Nix and LC3

For the coimmunoprecipitation of Nix with LC3, the pretreated *Nix*$^{-/-}$ and control platelets (3 × 10^8/mL) were incubated in Pierce immunoprecipitation cell lysis buffer including phosphatase and protease inhibitor cocktails (Thermo Scientific) on ice for 30 minutes. The platelet samples were further incubated with anti-Nix antibody or anti-LC3 antibody on ice for 2 hours, and then they were further incubated with protein G beads at 4°C overnight. The bead-bound platelet proteins were harvested by centrifugation for 2 minutes at 3000*g* at 4°C, and then the proteins were washed with the immunoprecipitation solution and extracted. The extracted proteins were analyzed by western blotting by using the indicated antibodies.

Analysis of mouse tail-bleeding time

The tail-bleeding time assay was performed on mice as described previously.[32,40] Briefly, all mice were anesthetized with an intraperitoneal injection of avertin at a dose of 2.5% (10 mL/kg; 100% [wt/vol] tribromoethyl alcohol in tertiary amyl alcohol) in phosphate-buffered saline buffer. A razor blade was used to transect the tails of the *Nix*$^{-/-}$ and control mice 3 mm from the tail tip, and the tails were immediately immersed in phosphate-buffered saline solutions at 37°C. The tail-bleeding time was determined when the bleeding from the tail stopped for at least 10 seconds. Bleeding was stopped at the time point of 15 minutes.

Mouse models of carotid artery thrombosis induced by $FeCl_3$

The $FeCl_3$-induced carotid artery thrombosis model was constructed as described previously.[40] Briefly, all mice were anesthetized with an intraperitoneal injection of pentobarbital (40 mg/kg). The carotid arteries of *Nix*$^{-/-}$ and control mice at the age of 8 weeks were exposed and treated with filter paper soaked with 5% $FeCl_3$ for 120 seconds. The blood flow rate of the carotid artery was monitored from the time of $FeCl_3$ exposure during the subsequent 13 minutes using a small-animal transducer. When the carotid artery blood flow was <0.06 mL/min, it was scored as occlusion. The experimenters were blinded to the genotypes of the mice when conducting the experiments.

Flow cytometry analysis

Mitochondrial inner transmembrane potential of the pretreated platelets from 8-week-old *Nix*$^{-/-}$ and control mice was analyzed by flow cytometry using tetramethylrhodamine ethyl ester perchlorate (TMRE). Briefly, the washed *Nix*$^{-/-}$ and control platelets (3 × 10^8/mL) were pretreated with FCCP (5 μM) or vehicle control DMSO at room temperature for 120 minutes, and then they were further incubated with TMRE (at a final concentration of 100 nM) at 37°C for 20 minutes in the dark. Finally, mitochondrial inner transmembrane potential was detected by flow cytometry as described previously.[6]

Levels of mitochondrial ROS in resting platelets were analyzed by using Mito-SOX following the manufacturer's instructions (Beyotime). Briefly, the pretreated platelets were treated with Mito-SOX (0.1 μM) at 37°C for 20 minutes in the dark. After washing with MTB 3 times, flow cytometry was used to analyze the Mito-SOX fluorescence intensity of the above platelets.

For the analysis of P-selectin surface expression, platelets from 8-week-old *Nix*$^{-/-}$ and control mice were pretreated with FCCP (5 μM) or vehicle control DMSO at room temperature for 120 minutes. The pretreated platelets stimulated with thrombin (0.05 U/mL) were then incubated with anti–P-selectin antibody or control IgG for 30 minutes at room temperature, and then they were further treated with FITC-GAM for 30 minutes at room temperature and analyzed by flow cytometry.

Activation of $\alpha_{IIb}\beta_3$ on platelets was analyzed by using an antibody (clone/isotype: JON/A/Rat [Wistar] IgG2b) against the active $\alpha_{IIb}\beta_3$. The above pretreated platelets were further stimulated with thrombin (0.05 U/mL) and incubated with the antibody against the active $\alpha_{IIb}\beta_3$ for 20 minutes at room temperature. The incubated platelets were fixed in cold paraformaldehyde (1%) at 4°C for 30 minutes, and finally the platelet samples were analyzed by flow cytometry.

Metabolic assay

Oxygen consumption rate (OCR) of platelets was examined as described previously.[5,6] Briefly, platelets (3 × 10^8/mL) were resuspended in Dulbecco's modified Eagle medium (Sigma) containing HEPES (0.02 M; ICN Biomedicals Inc) in the presence of 0.02 U/mL apyrase. Platelets (200 μL, 3 × 10^7/mL) were then plated on the XFp microplate well and incubated at 37°C for 20 minutes. The assay solution was supplemented with 2.5 M D-glucose, 1 mM glutamine, and 1 mM pyruvate for OCR measurement. The OCR of platelets was measured under basal condition, or in the presence of oligomycin (0.25 μM), FCCP (5 μM), rotenone and antimycin (1 μM) consecutively according to the instruction from the company (Seahorse kit).[6] Five individual basal measurements were done for each assay and 3 independent measurements were done after each treatment.

To analyze the ATP level in platelet lysates, an ATP Bioluminescence Assay kit HS II (Roche) was used following the directions of the manufacturer as described previously.[6]

Mitophagy analysis by electron microscopy

Morphological mitophagy of platelets was examined by electron microscopy. Briefly, platelets prepared from 8-week-old *Nix*$^{-/-}$

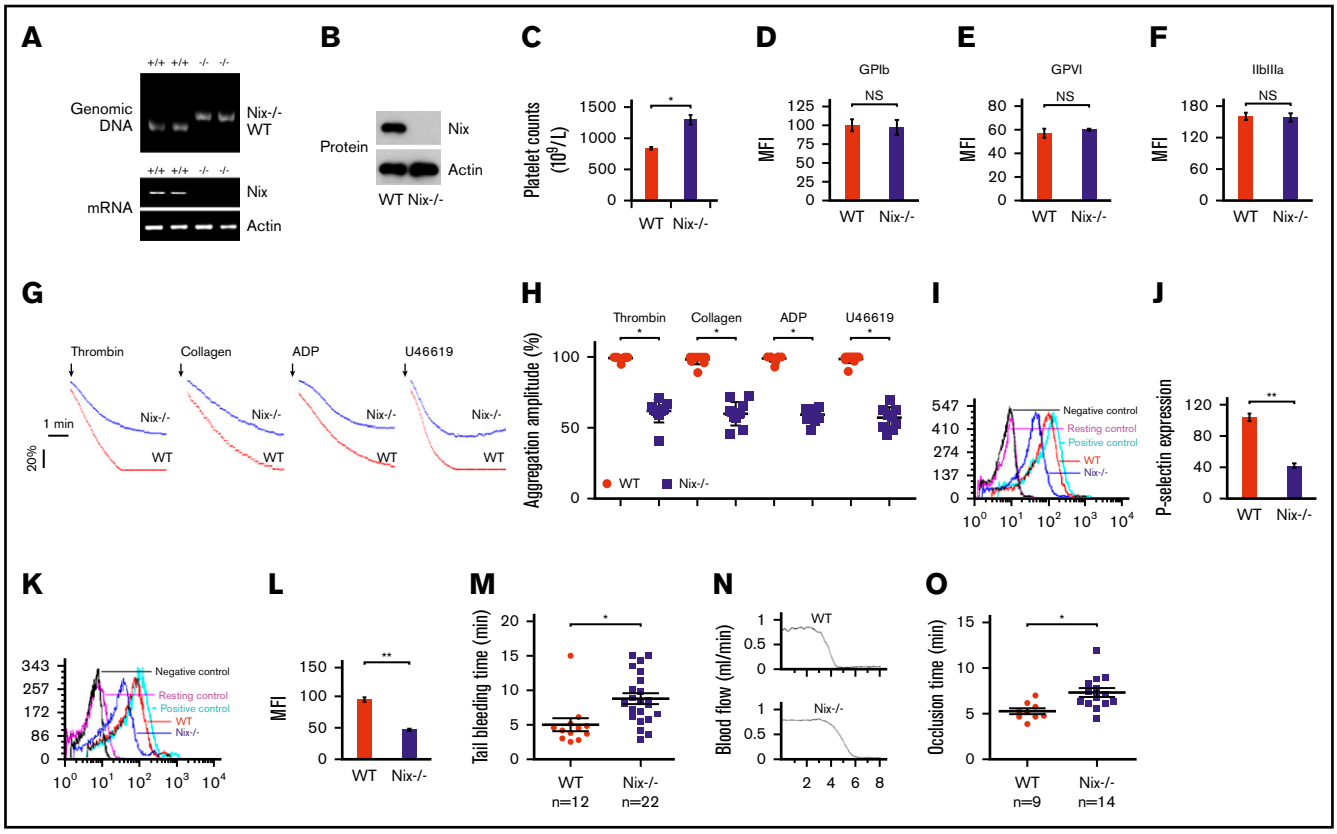

Figure 1. Genetic ablation of *Nix* impairs platelet activation. (A-B) Characterization of *Nix* knockout ($Nix^{-/-}$) mice by polymerase chain reaction (A) and western blotting (B). (C) Platelet counts from $Nix^{-/-}$ mice and WT controls (WT) were illustrated. Student *t* test. (D-F) Platelet membrane receptors GPIb (D), GPVI (E), and GPIIbIIIa (F) were analyzed by flow cytometry using specific antibodies. Student *t* test. (G-H) Platelet aggregation induced by thrombin, collagen, ADP, and U46619 was monitored. (G) Baseline of platelet aggregation trace was indicated with arrowhead. (H) The aggregation amplitudes were analyzed (n = 11). Student *t* test. (I-J) P-selectin surface expression of platelets treated with 0.05 U/mL α-thrombin was examined by flow cytometry using anti–P-selectin antibody, and negative controls (IgG control), resting platelet controls, and positive controls (A23187-treated platelets) have been included (I); statistical analysis of the data is shown in panel J. Student *t* test. (K-L) Platelet activation of platelets treated with 0.05 U/mL α-thrombin was detected by flow cytometry using an antibody against the active $\alpha_{IIb}\beta_3$, and negative controls (IgG control), resting platelet controls, and positive controls (A23187-treated platelets) have been included (K); statistical analysis of the data is demonstrated in panel L. Student *t* test. (M) Comparison of tail-bleeding time in $Nix^{-/-}$ mice and WT controls. Nonparametric test. (N-O) The occlusion times in the $FeCl_3$-induced thrombus models in $Nix^{-/-}$ mice and WT controls (N); statistical analysis of the data using the nonparametric test is shown in panel O. *$P < .05$; **$P < .01$. n = 9 for each group if it is not stated in the figures. MFI, mean fluorescence intensity; mRNA, messenger RNA; NS, not significant.

and control mice were pretreated with FCCP and fixed with glutaraldehyde (2.5%) for 120 minutes at room temperature. Mitophagy analysis by electron microscopy was performed as described previously[6] using a 120-kV JEOL electron microscope at 80 kV.

Radiation chimeras and bone marrow transplantation assay

The protocols to generate radiation chimeras and perform bone marrow transplantation assays have been described previously.[41] Briefly, WT mice and $Nix^{-/-}$ mice were firstly subjected to γ-irradiation at a dose of 8.5 Gy from a ^{60}Co source (Institute of Zoology, Chinese Academy of Sciences), and then the prepared bone marrow cells (5×10^6 cells per mice) were injected into the tail vein of the irradiated mice. Four weeks after transplantation, the reconstituted mice were tested to analyze $FeCl_3$-induced thrombosis of the carotid artery, tail-bleeding time, and platelet activation as described previously.[6,40,42]

Analysis of platelet life span and adoptive platelet transfer assay

The platelet life span assay and adoptive platelet transfer assay were conducted as described previously.[7,43] Briefly, $Nix^{-/-}$ and WT mice were injected IV with *N*-hydroxysuccinimide ester (NHS)-biotin (300 μg per 20-mg mouse). Whole blood was collected at various time points (0 hours, 24 hours, 48 hours, 72 hours, 96 hours, 120 hours, and 144 hours) and platelets were isolated and prepared. Flow cytometry was used to analyze platelet life span.

For the analysis of adoptive platelet transfer, $Nix^{-/-}$ and WT mice were firstly injected with NHS-biotin IV, and then platelets were isolated and resuspended in saline solution 30 minutes after the injection. Finally, the prepared platelets were IV injected into recipient mice of the same or different genotypes. Biotinylated platelets were analyzed by flow cytometry.[44-47]

For the detection of platelet mitophagy of the biotinylated platelets, the whole blood of the mice with NHS-biotin injection was collected

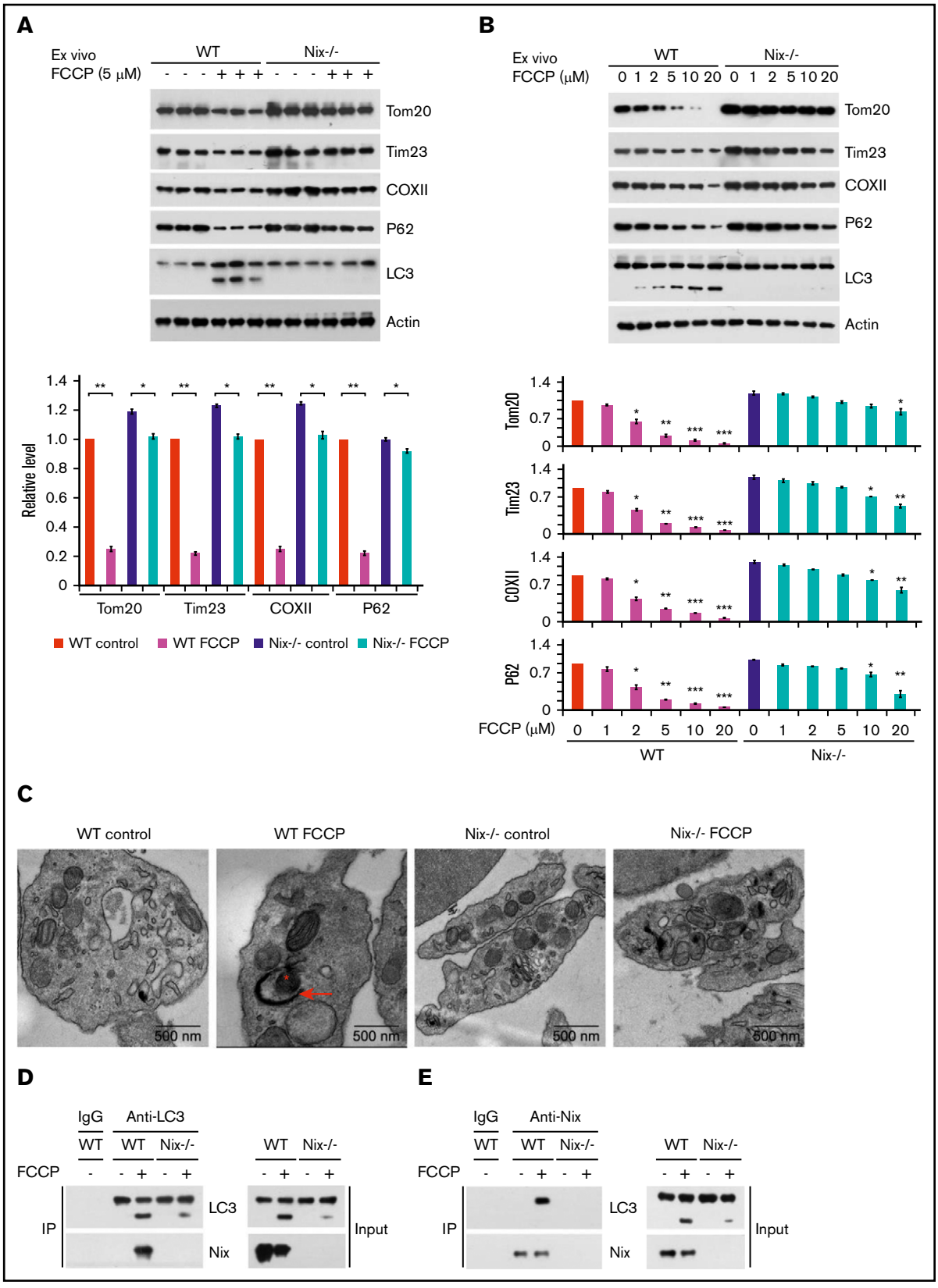

Figure 2. Nix induces mitochondrial autophagy in platelets in response to FCCP. Platelets were isolated from the blood of *Nix*$^{-/-}$ mice and WT mice. (A-B) Platelets (3×10^8/mL) were treated with FCCP at 5 μM in panel A or at the indicated concentrations in panel B at room temperature for 2 hours, and the samples were subjected to western blotting analysis using the indicated antibodies. (A) Each lane in the same treatment of mouse represents a different mouse and 3 independent experiments with a

and washed platelets were prepared. The isolated platelets were further incubated with FITC-avidin and sorted by flow cytometry as described previously.[44-47]

Statistical analysis

All data analysis was performed with GraphPad PRISM version 5.01 (GraphPad Software, Inc) and SPSS 18.0 software (SPSS Inc). Sample size was not statistically calculated. Data are presented as mean ± standard error of the mean. The normality of distribution of the data sets was tested by using the Kolmogorov-Smirnov test. Two data groups with normal distribution were analyzed by using the 2-sided unpaired Student *t* test. Two data groups with abnormal distribution were analyzed by using the nonparametric test. For the analysis of the multiple group comparisons, 1-way analysis of variance (ANOVA) with the Bonferroni post hoc test was used. The Mann-Whitney *U* test was used for the analysis of nonparametric data (*$P < .05$; **$P < .01$; ***$P < .001$).

Results

Genetic ablation of *Nix* impairs platelet activation

To explore the role of Nix in platelets, we used $Nix^{-/-}$ mice that were generated as described previously.[36] Successful targeting of the *Nix* locus was confirmed at the genomic DNA, messenger RNA, and protein levels (Figure 1A-B).[36] Interestingly, there were increased platelet counts in the $Nix^{-/-}$ mice (Figure 1C), but no difference in platelet size (mean platelet volume) (data not shown). Flow cytometry and western blot studies revealed similar surface expression levels of platelet GP receptors, including GPIbα, GPVI and GPIIbIIIa (also termed as $\alpha_{IIb}\beta_3$), protease-activated receptors 3/4, and $P2Y_{12}$, between genotypes (Figure 1D-F; supplemental Figure 1). As previously reported, there were decreased numbers of red blood cells and no change in white blood cell counts (supplemental Figure 2A-B) in $Nix^{-/-}$ mice.[14,32,36,37]

Next, we examined platelet activation under various stimuli and found that genetic ablation of *Nix* inhibited platelet aggregation (Figure 1G-H). P-selectin surface expression and activation of $\alpha_{IIb}\beta_3$ are the hallmarks of platelet activation. Flow cytometric analysis using anti–P-selectin antibody revealed that platelet activation marker P-selectin was significantly higher in WT platelets than that of the $Nix^{-/-}$ group upon treatment with thrombin (Figure 1I-J). Consistent with this, the binding of the antibody JON/A to the activated $\alpha_{IIb}\beta_3$ in the WT group was significantly higher than in the $Nix^{-/-}$ group (Figure 1K-L). Taken together, these results suggest that *Nix* knockout impaired platelet activation without affecting the expression of platelet glycoproteins such as GPIb, GPVI, and $\alpha_{IIb}\beta_3$.

Platelet activation leads to blood clotting by formation of a platelet plug, which is a key step in hemostasis and thrombosis. Thus, the role of Nix in platelets was further verified by using tail bleeding and $FeCl_3$-induced carotid artery thrombosis models in vivo. The tail-bleeding time in $Nix^{-/-}$ mice was increased approximately twofold compared with the WT control group (Figure 1M), suggesting that Nix plays an integral role in platelet activation and hemostasis. Consistent with this, the complete occlusion time in carotid artery thrombosis was significantly longer in $Nix^{-/-}$ mice than in the control mice (Figure 1N-O). Taken together, these data indicate that *Nix* knockout results in increased platelet count, but decreased platelet activation, and impaired hemostasis and thrombosis.

Nix regulates mitophagy in platelets in response to FCCP

It is well known that Nix harbors a conserved LIR motif that interacts with LC3 to mediate mitophagy.[33] *Nix* knockout may result in the accumulation of functionally compromised mitochondria, leading to impaired platelet activation. We thus first examined whether Nix plays a role in platelet mitophagy. Platelets from $Nix^{-/-}$ mice and controls were treated with FCCP, a mitochondrial uncoupling agent, to induce mitophagy. As shown in Figure 2A-B, FCCP treatment reduced the levels of multiple mitochondrial proteins (the inner membrane proteins COXII and Tim23 and the outer membrane protein Tom20), and decreased the level of the autophagy adaptor protein P62 (SQSTM1) in WT platelets in a dose-dependent manner. Lipidation of the autophagy protein LC3 was also induced by FCCP. These biochemical hallmarks of mitophagy were clearly blocked in $Nix^{-/-}$ platelets, indicating a crucial role of Nix in platelet mitophagy induced by FCCP.

Morphological analysis of FCCP-treated WT platelets by electron microscopy revealed typical structures associated with mitophagy, for example, mitochondria enclosed within double-membrane mitophagosomes (Figure 2C). The mitophagosome phenotype was greatly reduced in FCCP-treated platelets from $Nix^{-/-}$ mice (Figure 2C). It was reported that Nix mediates mitophagy by interacting with LC3 through its LIR domain in HeLa cells.[33] As expected, coimmunoprecipitation analysis showed that Nix interacts with LC3 strongly in FCCP-treated WT platelets, and this interaction was blocked in $Nix^{-/-}$ platelets (Figure 2D-E). Taken together, these data demonstrated that Nix mediates platelet mitophagy through its direct interaction with LC3.

Nix-mediated platelet mitophagy regulates platelet mitochondrial quality and platelet activation

We next investigated whether mitophagy mediated by Nix is also involved in regulation of mitochondrial quality and function in platelets by using the uncoupler of mitochondrial oxidative phosphorylation FCCP to induce mitophagy. OCR of platelets was measured under basal condition, or in the presence of oligomycin, FCCP, rotenone, and antimycin, respectively. The results of seahorse analysis revealed

Figure 2. (continued) total of 9 mice were used. (B) Three mice of WT and 3 mice of $Nix^{-/-}$ were used and the platelets were pooled in 1 experiment, and 3 independent experiments with a total of 9 mice were used. The grayscale values of all the bands were measured with ImageJ software and the statistical data are illustrated. ANOVA was used. (C) Platelets were treated as described in panel A, and platelet mitophagy was detected by electron microscopy. Mitophagy phenomenon of mitochondria enclosed in autophagosomes was quantitated, and the data demonstrated that 4 of 318 mitochondria were observed within the autophagosomes in 60 WT platelets treated with FCCP and 0 of 387 mitochondria were observed within the autophagosomes in 60 $Nix^{-/-}$ platelets treated with FCCP. (D-E) Analysis of the interaction between Nix and LC3 by coimmunoprecipitation. The IgG-treated sample served as a control; n = 9 for each group. Red asterisk, mitochondrion. Red arrow, double-membrane autophagic structures (mitophagosomes).

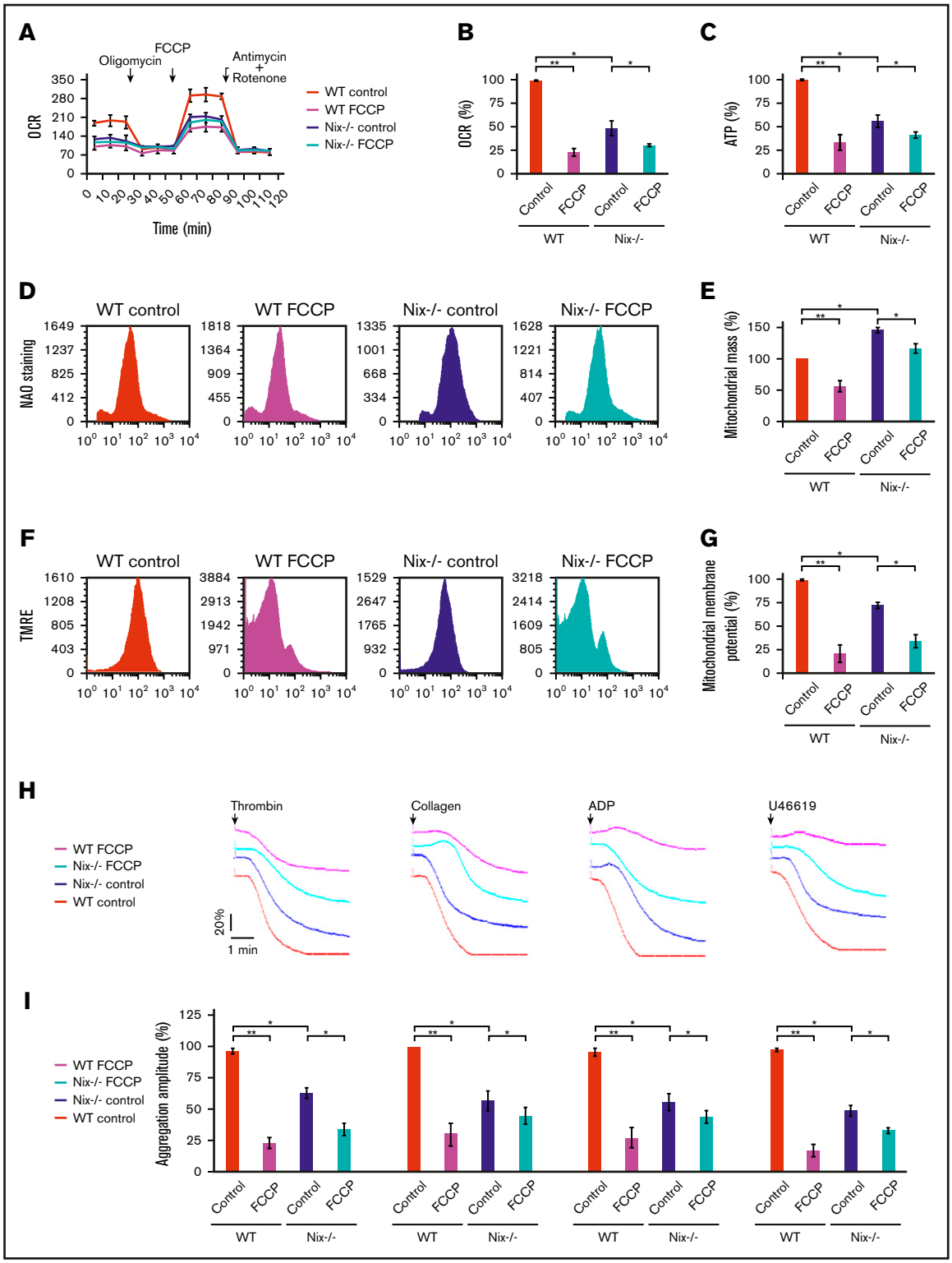

Figure 3. Nix-mediated-platelet mitophagy regulates platelet mitochondrial quality and platelet activity. Platelets were isolated from the blood of *Nix*$^{-/-}$ mice and WT mice. The prepared platelets (3×10^8/mL) were treated with FCCP (5 μM) for 2 hours at room temperature, and then analyzed for mitochondrial quality and platelet activation. (A-B) OCR of platelets from *Nix*$^{-/-}$ mice and WT controls (WT) was measured by Seahorse analysis (A); statistical analysis of the data are presented in panel B. (C) Statistical analysis of the ATP production capacity of platelets from *Nix*$^{-/-}$ mice and WT controls. (D-E) Platelets were treated with the selective mitochondrial dye nonyl acridine orange (NAO) and analyzed by flow cytometry to determine the mitochondrial mass (D). Statistical analysis of the data are presented in panel E. (F-G) Mitochondrial membrane potential was detected by flow cytometry using TMRE staining (F); statistical analysis of the data are shown in panel G. (H-I) Platelet aggregation induced by thrombin, collagen, ADP, and U46619 were detected (H) and the aggregation amplitudes were analyzed (I). Baseline of platelet aggregation trace was indicated with

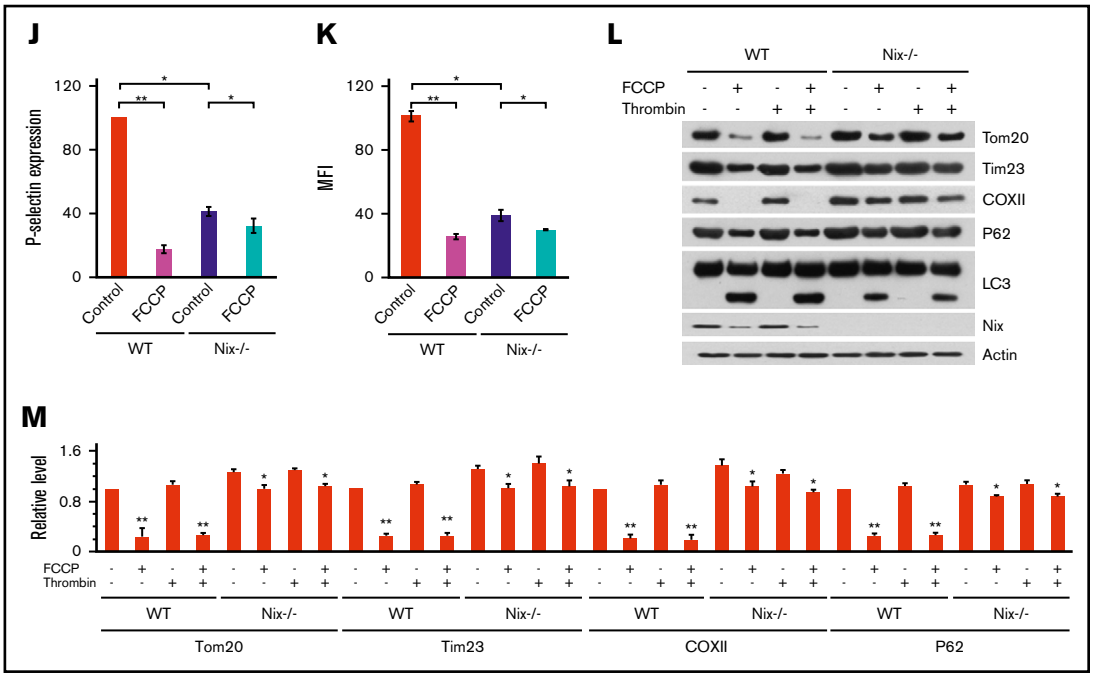

Figure 3. (Continued) arrowhead. (J-K) P-selectin surface expression and $\alpha_{IIb}\beta_3$ activation were analyzed on platelets stimulated with 0.05 U/mL α-thrombin by flow cytometry using antibodies against P-selectin (J) and the active $\alpha_{IIb}\beta_3$ (K), respectively. Statistical analysis of the data are shown. (L-M) Platelet mitophagy was analyzed by western blotting using the indicated antibodies (L). (M) The grayscale values of all the bands were measured with ImageJ software and the statistical data are illustrated. ANOVA was used. $^*P < .05$; $^{**}P < .01$; n = 6 for each group.

that basal and maximal OCR and ATP production capacity were reduced in *Nix*$^{-/-}$ platelets compared with WT controls (Figure 3A-C control groups). This indicates that mitochondrial respiration is impaired in the absence of Nix. Moreover, FCCP pretreatment induced a dramatic decrease in basal and maximal mitochondrial respiration, which was largely abrogated in *Nix*$^{-/-}$ platelets (Figure 3A-B). These data indicated that FCCP-induced mitophagy in WT platelets significantly eliminated mitochondria and thereby reduced mitochondrial function, which is in agreement with the extensive degradation of mitochondrial proteins (ie, Tom20, Tim23, and COXII) (Figure 2A-B). However, the compromised mitochondrial functions in *Nix*$^{-/-}$ platelets were more likely to result from accumulation of defective mitochondria that escaped from mitophagy, as evidenced by the increased mitochondrial mass by flow cytometry using nonyl acridine orange, which can label phospholipids on the surface of mitochondria and evaluate the quantity of mitochondria, increased mitochondrial ROS, and reduction of mitochondrial membrane potential by flow cytometry using TMRE, which can selectively label healthy and living mitochondrion and evaluate the mitochondrial membrane potential of resting platelets (Figure 3D-G; supplemental Figure 3). Collectively, these data show that Nix-mediated mitophagy regulates both mitochondrial quality and functional integrity in platelets.

Next, we sought to explore whether Nix-mediated mitophagy regulates platelet activation. Exposure of WT platelets to FCCP significantly inhibited platelet activation (Figure 3H-K). In contrast, the activation of platelets from *Nix*$^{-/-}$ mice was less affected by FCCP treatment, suggesting a specific role of Nix-mediated mitophagy in platelet activation. The significant differences in platelet activation between WT and *Nix*$^{-/-}$ mice were in accordance with the different degree of platelet mitophagy (Figure 3L-M). Collectively, these data demonstrate that Nix-mediated mitophagy regulates platelet activation.

Platelet-autonomous role (acting on platelets, but not other cells) of Nix in platelet activation

Nix$^{-/-}$ mice are conventional knockouts, and *Nix* function is absent from the whole body. Therefore, we performed bone marrow transplantation to exclude any effects of the interactions between platelets and other cells such as vascular endothelial cells. Bone marrow derived from *Nix*$^{-/-}$ or WT animals were transplanted into recipient mice (*Nix*$^{-/-}$ or WT), which were pretreated with radiograph irradiation at a single dose of 8.5 Gy. The protein levels of Nix in the platelets after the bone marrow transplantation were evaluated by immunoblotting assays (Figure 4I).

As expected, these WT mice carrying KO bone marrow–derived cells (BMDCs) from *Nix*$^{-/-}$ mice showed significantly longer tail-bleeding times (439 ± 24 seconds; n = 8; $P = .00076$) than control WT animals (221 ± 31 seconds; n = 8) (Figure 4A). The bleeding time in WT mice with *Nix*$^{-/-}$ BMDCs was similar to that in *Nix*$^{-/-}$ mice. In contrast, transplantation of WT bone marrow into the *Nix*$^{-/-}$ mice rescued the hemostasis deficiency (Figure 4A). Similar results were observed in the $FeCl_3$-induced arterial thrombosis model (Figure 4B). These data indicate that *Nix* gene expression in platelets indeed affects thrombosis and hemostasis in vivo, and loss of *Nix* in BMDCs, presumably the platelets, plays an important role in the impaired arterial thrombosis in the *Nix*$^{-/-}$ mice.

Measurements of thrombin-induced platelet activation, including platelet aggregation, P-selectin surface expression, and activation

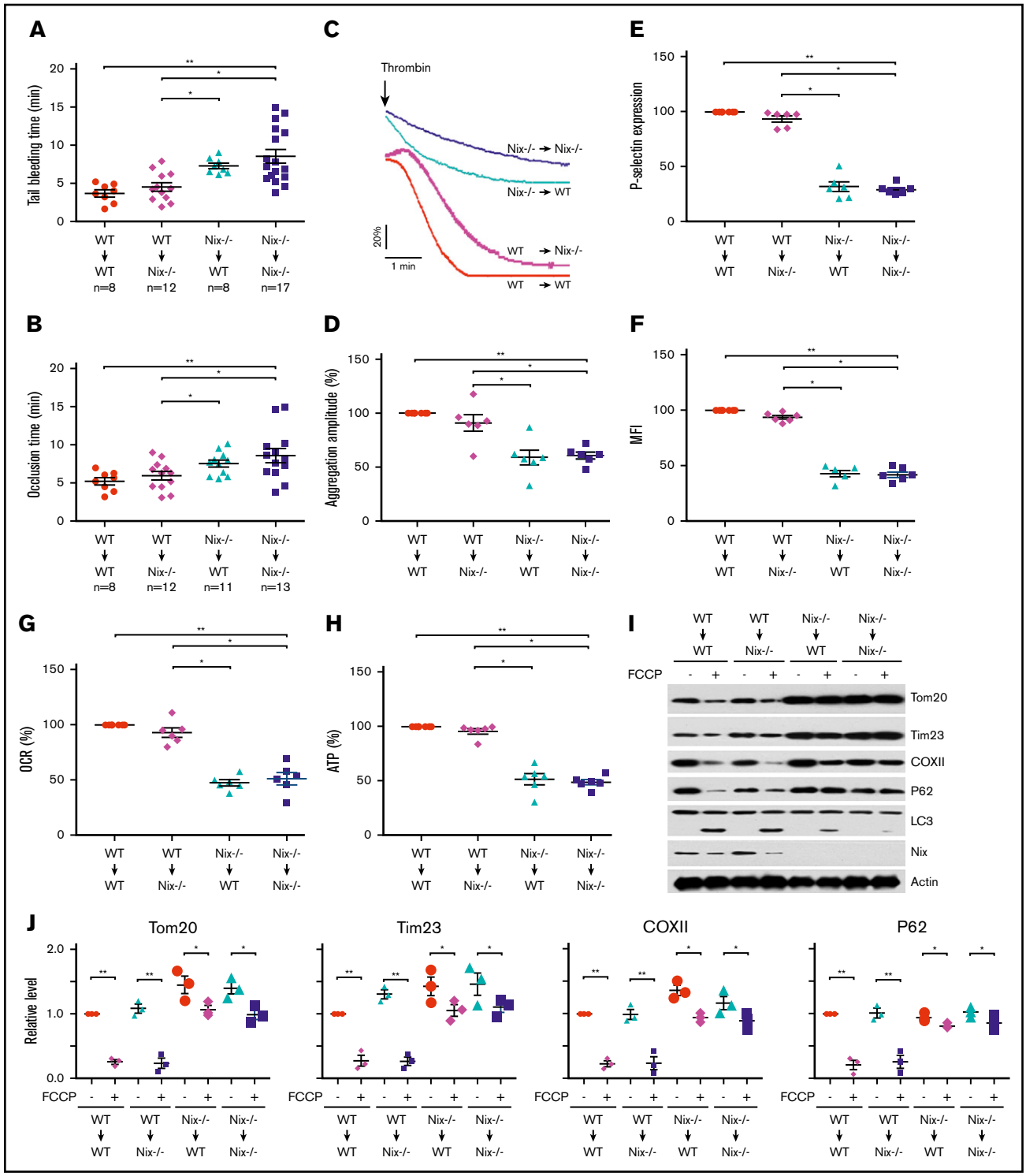

Figure 4. Transplantation of bone marrow cells from WT mice rescues the impaired platelet functions of *Nix*$^{-/-}$ mice Bone marrow was isolated from *Nix*$^{-/-}$ mice and WT mice. The prepared bone marrow samples were transplanted into recipient mice as indicated in the figures. (A) Statistical analysis of tail-bleeding times of the transplanted *Nix*$^{-/-}$ mice and WT mice. (B) Statistical analysis of occlusion time in the $FeCl_3$-induced thrombus model in transplanted *Nix*$^{-/-}$ mice and WT mice. (C-D) Platelet aggregation induced by thrombin was monitored (C) and the aggregation amplitudes were analyzed (D). Baseline of platelet aggregation trace was indicated with arrowhead. (E-F) P-selectin surface expression and $\alpha_{IIb}\beta_3$ activation were analyzed by flow cytometry in platelets stimulated with 0.05 U/mL α-thrombin from the transplanted mice using antibodies against P-selectin (E) and the active $\alpha_{IIb}\beta_3$ (F), respectively. Statistical analysis of the data are shown. (G) OCR of the platelets from transplanted *Nix*$^{-/-}$ and WT mice. Mitochondrial OCR was measured by Seahorse analysis. (H) ATP production capacity of platelets from transplanted *Nix*$^{-/-}$ and WT mice. (I-J) Induction of mitophagy in FCCP-treated platelets from transplanted mice was detected by western blotting using the indicated antibodies (I). (J) The grayscale values of all the bands were measured with ImageJ software and the statistical data are illustrated. ANOVA was used. *$P < .05$; **$P < .01$; n = 6 for each group if it is not stated in the figures.

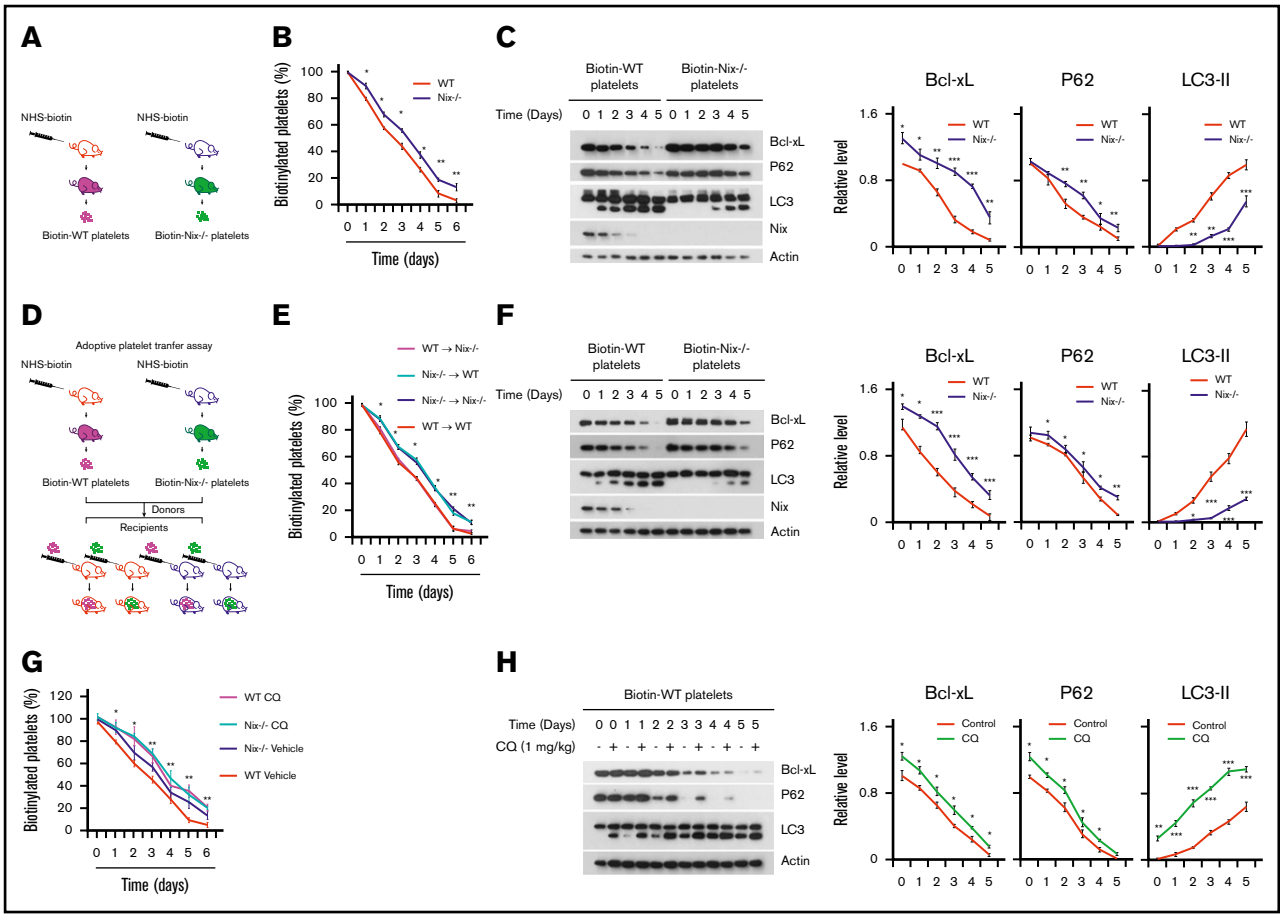

Figure 5. Knockout of *Nix* increases the life span of platelets by inhibiting the autophagic degradation of the mitochondrial protein Bcl-xL in vivo. (A-B) $Nix^{-/-}$ and WT mice were injected IV with NHS-biotin (A). Whole blood was collected at various time points and platelets were isolated and prepared. Flow cytometry was used to analyze the platelet life span. (B) The data were analyzed using CellQuest software (BD Biosciences). (C) Platelets were collected by cell sorting as described in panel A, and western blotting was used to analyze platelet mitophagy. (D-F) The adoptive platelet transfer assay was conducted as shown in panel D, and $Nix^{-/-}$ and WT mice were IV injected with NHS-biotin, 30 minutes after the injection, platelets were isolated and resuspended in saline solution. The prepared platelets were then IV injected into recipient mice as indicated. Biotinylated platelets were analyzed by flow cytometry. (E) Data from 3 separate experiments are shown as mean ± standard error of the mean. (F) Western blotting was used to analyze mitophagy of the biotin-labeled platelets from the recipient mice. (G-H) $Nix^{-/-}$ and WT mice were injected IV with NHS-biotin, and the pretreated mice were further injected intraperitoneally with chloroquine (CQ; 1 mg/kg). Whole blood was collected at various time points and platelets were isolated and prepared. Flow cytometry was used to analyze the platelet life span. (G) The data were analyzed using CellQuest software (BD Biosciences). (H) Platelets were collected as described in panel A, and western blotting was used to analyze platelet mitophagy. (C,F,H) 6 mice of WT and 6 mice of $Nix^{-/-}$ were used in 1 experiment, and 3 independent experiments with total of 18 mice were used. The grayscale values of all the western blot bands were measured with ImageJ software and the statistical data are illustrated. Student *t* test. $^{*}P < .05$; $^{**}P < .01$; $^{***}P < .001$.

of $\alpha_{IIb}\beta_3$, further confirmed that transplantation of WT bone marrow into $Nix^{-/-}$ mice significantly increased the activities of the platelets (Figure 4C-F). Finally, transplantation of WT bone marrow cells fully restored platelet mitochondrial quality as revealed by mitochondrial respiration (Figure 4G-H) and mitophagy flux (Figure 4I-J) in $Nix^{-/-}$ mice. The western blot results of the transplantation of bone marrow cells (Figure 4I) indicate that platelet Nix is important in FCCP-induced platelet mitophagy, which is independent of recipient mice or other blood cells.

To further exclude the interference of other cells including red blood cells, the platelet transfer experiment was used and the results demonstrated that injection of WT platelets into $Nix^{-/-}$ mice could significantly rescue the hemostasis detects of the $Nix^{-/-}$ mice in the tail-bleeding time assay (supplemental Figure 4). Taking these results together, we conclude that *Nix* deficiency in platelets plays an important role in the compromised platelet activity and thrombosis function in vivo.

A Nix–Bcl-xL axis regulates platelet life span

The increased platelet count in $Nix^{-/-}$ mice (Figure 1C) may result from increased production of platelets from megakaryocytes, from decreased platelet apoptosis, or from increased platelet life span. We analyzed bone marrow cells from $Nix^{-/-}$ mice and WT mice by flow cytometry using antibodies against GPIb-phycoerythrin and CD41-FITC and found no significant difference in megakaryocyte numbers (supplemental Figure 5). Although Nix is also involved in apoptosis in various cells, we observed no significant apoptosis of platelets from the $Nix^{-/-}$ mice at baseline, whereas $Nix^{-/-}$ platelets

displayed less apoptotic markers compared with that of WT platelets upon ABT-737 treatment (supplemental Figure 6). We then performed the platelet clearance assay to address the life span issue.

WT and *Nix*$^{-/-}$ mice were injected IV with NHS-biotin to pulse label blood cells with biotin, and then platelets were isolated from whole blood at various time points. Biotin-labeled platelets were detected by flow cytometry to analyze biotin labeling on platelets, which revealed that loss of *Nix* increased platelet life span in vivo (Figure 5A-B). To verify that the changes in platelet life span were due to the intrinsic properties of the platelets, reciprocal adoptive transfer studies were performed. As shown in Figure 5D-E, the *Nix*$^{-/-}$ platelets were cleared more slowly than WT platelets in both WT and *Nix*$^{-/-}$ recipients, with half-lives comparable to those observed in *Nix*$^{-/-}$ mice. Conversely, the clearance of WT platelets was similar in WT and *Nix*$^{-/-}$ recipients, with similar half-lives similar to those in WT mice. These data demonstrated that the life span of platelets is solely determined by the platelet genotype regardless of the genotypes of the recipients.

Next, we further explored the underlying mechanism of the increased life span of *Nix*$^{-/-}$ platelets. It has been reported by Kile's group that Bcl-xL functions as a molecular clock to control the life span of platelets.[7] Therefore, we sorted the pulse-labeled biotinylated platelets by flow cytometry at different time points after the NHS-biotin injection, and subjected them to western blot analysis. The level of Bcl-xL in WT platelets decreased in a time-dependent manner in vivo, and this was accompanied by an increased level of autophagy, which were significantly prevented in *Nix*$^{-/-}$ platelets in both naive mice (Figure 5C), and adoptive transfused mice receiving platelet transfers (Figure 5F). In addition, inhibiting autophagy by chloroquine significantly increased the life span by preventing degradation of Bcl-xL in vivo (Figure 5G-H). These data strongly suggest that Nix-mediated mitophagy also determines platelet life span by inhibiting the autophagic degradation of the mitochondrial protein Bcl-xL in vivo.

Discussion

In the present study, we have provided evidence showing that Nix controls platelet activation, hemostasis, and thrombosis by regulating mitophagy and mitochondrial quality in platelets. *Nix* deficiency caused accumulation of functionally compromised mitochondria in platelets, leading to impaired platelet activation, prolonged tail-bleeding time, and attenuated arterial thrombosis in the $FeCl_3$-induced carotid arterial injury model. Interestingly, *Nix* deficiency did not incur changes of number of α-granules and dense granules (supplemental Figures 7 and 8), nor the platelet secretion (supplemental Figure 9), although platelet integrin activation was impaired upon stimulation with agonists (Figure 1; supplemental Figure 10). Transplantation of WT bone marrow cells into *Nix*-deficient mice significantly rescued defects in platelet function and thrombosis, and injection of WT platelets into *Nix*$^{-/-}$ mice could significantly rescue the hemostasis detects of the *Nix*$^{-/-}$ mice in the tail-bleeding time assay (supplemental Figure 4), suggesting a platelet-autonomous role (acting on platelets, but not other cells) of Nix in platelet activation. We propose that there is a possibility that some mitochondria in *Nix* KO are born defective and some mitochondria become defective over time due to defective mitophagy in platelets with aging (supplemental Figure 11), although it remains to be investigated. Furthermore, our results imply that targeting platelet mitophagy may represent a new antithrombotic strategy.

It has been reported that mitophagy is critical for maintaining mitochondrial quality, energy metabolism, and organ function in mitochondrion-dense cells, including neurons, cardiomyocytes, and skeletal muscle cells.[10,16] However, the role of mitophagy in platelets, which contain only a few mitochondria, remains incompletely understood. We were the first to report that platelets undergo FUNDC1-mediated mitophagy in response to hypoxia, which is critical to ischemic adaptation.[6] In the present study, we showed that Nix regulates mitophagy flux as a housekeeping process to maintain mitochondrial quality in platelets. Loss of *Nix* in platelets leads to accumulation of damaged mitochondria, excessive mitochondrial ROS production (supplemental Figure 3), and impaired platelet function. Nix/BNIP3L is a BH3-only protein that plays important roles in both mitophagy and apoptosis.[14,32,33] It is well recognized that genetic ablation of *Nix* causes defective maturation of erythrocytes and leads to anemia in both mice and humans.[14,33,36,37] Our findings thus suggest that Nix has a new role in controlling basal mitophagy, mitochondrial quality, platelet function, thrombosis, and hemostasis in platelets. It is notable that *Nix*-deficient platelets also exhibited mitophagy in response to FCCP, although the degree of mitophagy was markedly lower than that of the WT mice, which suggests that other mitophagy pathways also play roles in the absence of Nix. Further studies using *Nix* and *Fundc1* double knockout mice will help to address the role of mitophagy in platelet functions.

An important aspect of our work relates to the identification of Nix as a critical regulator of platelet life span. We showed that Nix regulates Bcl-xL protein levels, likely through autophagic degradation. Bcl-xL is a molecular clock protein known to regulate platelet life span.[7,8] We found that loss of Nix increases Bcl-xL protein levels in platelets, and this in turn may prolong platelet life span. Inhibition of autophagy by chloroquine partially inhibits mitophagy in platelets and enhances platelet life span. It is also possible that Nix, a known BH3-containing protein, is able to antagonize Bcl-xL activity, thus decreasing life span. Given the clinical significance of platelet count and platelet transfusion, our finding that Nix controls platelet counts and life span holds great potential for platelet storage and therapeutic applications. In conclusion, our data demonstrate that Nix mediates platelet mitophagy, and deficiency of *Nix* results in dysfunctional mitochondria and impaired platelet activation. Our results help to link Nix-mediated mitophagy to platelet biology, and also suggest that targeting the platelet mitophagy receptor Nix may represent a new antithrombotic strategy.

Acknowledgments

The authors are grateful to all laboratory members for useful discussions. The authors thank Xiaoping Du from the University of Illinois at Chicago and Wei Li from Capital Medical University for their kind suggestions about the experiments or critical comments on the manuscript. The authors thank Yingchun Hu, He Ren, Guopeng Wang, Junlin Teng, and Chuanmao Zhang at Peking University and Pengyan Xia, Zhongshuang Lv, and Yinzi Ma at Institute of Zoology, Chinese Academy of Sciences for their technical advice and support with EM.

This work was supported by the Natural Science Foundation of China (31790404 [Q.C.], 31871392 [W.Z.], and 31671446 [L.L.]), the Special Fund for Strategic Pilot Technology Chinese Academy of Sciences (QYZDJ-SSW-SMC004) (Q.C.), the Beijing Natural Science Foundation (5192014) (W.Z.), and the National

Key Research and Development Program (2016YFA0500201) (Q.C.).

Authorship

Contribution: W.Z., X.L., L.L., and Q.C. designed the experiments, analyzed and interpreted the data and results, and wrote and edited the manuscript; W.Z. performed most of the experiments; Q.M. wrote and edited the manuscript; S.S. edited the manuscript; J.L. provided suggestions for the experimental design and important reagents, and edited and wrote the manuscript; P.A.N. made significant contributions with regard to the *Nix*$^{-/-}$ mice and edited the manuscript; and Y.Y. and W.L. conducted some experiments, analyzed data, and drafted and revised the manuscript.

Conflict-of-interest disclosure: The authors declare no competing financial interests.

ORCID profiles: S.S., 0000-0002-4595-0232; Q.C., 0000-0001-7539-8728.

Correspondence: Quan Chen, Tianjin Key Laboratory of Protein Science, College of Life Sciences, Nankai University, Tianjin 300071, China; e-mail: chenq@ioz.ac.cn; Lei Liu, State Key Laboratory of Membrane Biology, Institute of Zoology, Chinese Academy of Sciences, Beijing 100101, China; e-mail: liulei@ioz.ac.cn; or Weilin Zhang, State Key Laboratory of Membrane Biology, Institute of Zoology, Chinese Academy of Sciences, Beijing 100101, China; e-mail: zhangweilin@ioz.ac.cn.

References

1. Chen Y, Ruggeri ZM, Du X. 14-3-3 proteins in platelet biology and glycoprotein Ib-IX signaling. *Blood*. 2018;131(22):2436-2448.
2. Durrant TN, van den Bosch MT, Hers I. Integrin αIIbβ3 outside-in signaling. *Blood*. 2017;130(14):1607-1619.
3. Metharom P, Berndt MC, Baker RI, Andrews RK. Current state and novel approaches of antiplatelet therapy. *Arterioscler Thromb Vasc Biol*. 2015; 35(6):1327-1338.
4. Xu XR, Wang Y, Adili R, et al. Apolipoprotein A-IV binds αIIbβ3 integrin and inhibits thrombosis. *Nat Commun*. 2018;9(1):3608.
5. Schoenwaelder SM, Darbousset R, Cranmer SL, et al. 14-3-3ζ regulates the mitochondrial respiratory reserve linked to platelet phosphatidylserine exposure and procoagulant function [published correction appears in *Nat Commun*. 2017;8:16125]. *Nat Commun*. 2016;7:12862.
6. Zhang W, Ren H, Xu C, et al. Hypoxic mitophagy regulates mitochondrial quality and platelet activation and determines severity of I/R heart injury. *Elife*. 2016;5.
7. Mason KD, Carpinelli MR, Fletcher JI, et al. Programmed anuclear cell death delimits platelet life span. *Cell*. 2007;128(6):1173-1186.
8. Qi B, Hardwick JM. A Bcl-xL timer sets platelet life span. *Cell*. 2007;128(6):1035-1036.
9. Zhang W, Siraj S, Zhang R, Chen Q. Mitophagy receptor FUNDC1 regulates mitochondrial homeostasis and protects the heart from I/R injury. *Autophagy*. 2017;13(6):1080-1081.
10. Zhang W, Chen C, Wang J, Liu L, He Y, Chen Q. Mitophagy in cardiomyocytes and in platelets: a major mechanism of cardioprotection against ischemia/reperfusion injury. *Physiology (Bethesda)*. 2018;33(2):86-98.
11. Wallace DC. A mitochondrial paradigm of metabolic and degenerative diseases, aging, and cancer: a dawn for evolutionary medicine. *Annu Rev Genet*. 2005;39:359-407.
12. Wong YC, Ysselstein D, Krainc D. Mitochondria-lysosome contacts regulate mitochondrial fission via RAB7 GTP hydrolysis. *Nature*. 2018; 554(7692):382-386.
13. Liu L, Sakakibara K, Chen Q, Okamoto K. Receptor-mediated mitophagy in yeast and mammalian systems. *Cell Res*. 2014;24(7):787-795.
14. Sandoval H, Thiagarajan P, Dasgupta SK, et al. Essential role for Nix in autophagic maturation of erythroid cells. *Nature*. 2008;454(7201):232-235.
15. Pickrell AM, Youle RJ. The roles of PINK1, parkin, and mitochondrial fidelity in Parkinson's disease. *Neuron*. 2015;85(2):257-273.
16. Yamaguchi O, Murakawa T, Nishida K, Otsu K. Receptor-mediated mitophagy. *J Mol Cell Cardiol*. 2016;95:50-56.
17. Ohsumi Y. Historical landmarks of autophagy research. *Cell Res*. 2014;24(1):9-23.
18. Ouseph MM, Huang Y, Banerjee M, et al. Autophagy is induced upon platelet activation and is essential for hemostasis and thrombosis [published correction appears in *Blood*. 2015;126(17):2072]. *Blood*. 2015;126(10):1224-1233.
19. Banerjee M, Huang Y, Ouseph MM, et al. Autophagy in platelets. *Methods Mol Biol*. 2019;1880:511-528.
20. Feng W, Chang C, Luo D, et al. Dissection of autophagy in human platelets. *Autophagy*. 2014;10(4):642-651.
21. Paul M, Hemshekhar M, Kemparaju K, Girish KS. Aggregation is impaired in starved platelets due to enhanced autophagy and cellular energy depletion. *Platelets*. 2019;30(4):487-497.
22. Liu J, Song Q, Huang Y, Sun W, Lu D, Zhou B. R-lipoic acid overdosing affects platelet life span via ROS mediated autophagy. *Platelets*. 2018; 29(7):695-701.
23. Liu Y, Hu M, Luo D, et al. Class III PI3K positively regulates platelet activation and thrombosis via PI(3)P-directed function of NADPH oxidase. *Arterioscler Thromb Vasc Biol*. 2017;37(11):2075-2086.
24. Luo XL, Jiang JY, Huang Z, Chen LX. Autophagic regulation of platelet biology. *J Cell Physiol*. 2019;234(9):14483-14488.
25. Kim I, Rodriguez-Enriquez S, Lemasters JJ. Selective degradation of mitochondria by mitophagy. *Arch Biochem Biophys*. 2007; 462(2):245-253.

26. Wei Y, Chiang WC, Sumpter R Jr, Mishra P, Levine B. Prohibitin 2 is an inner mitochondrial membrane mitophagy receptor. *Cell*. 2017; 168(1-2):224-238.e10.

27. Gong G, Song M, Csordas G, Kelly DP, Matkovich SJ, Dorn GW II. Parkin-mediated mitophagy directs perinatal cardiac metabolic maturation in mice. *Science*. 2015;350(6265):aad2459.

28. Murakawa T, Yamaguchi O, Hashimoto A, et al. Bcl-2-like protein 13 is a mammalian Atg32 homologue that mediates mitophagy and mitochondrial fragmentation. *Nat Commun*. 2015;6:7527.

29. Gatica D, Lahiri V, Klionsky DJ. Cargo recognition and degradation by selective autophagy. *Nat Cell Biol*. 2018;20(3):233-242.

30. Liu L, Feng D, Chen G, et al. Mitochondrial outer-membrane protein FUNDC1 mediates hypoxia-induced mitophagy in mammalian cells. *Nat Cell Biol*. 2012;14(2):177-185.

31. Zhou H, Li D, Zhu P, et al. Melatonin suppresses platelet activation and function against cardiac ischemia/reperfusion injury via PPARγ/FUNDC1/ mitophagy pathways. *J Pineal Res*. 2017;63(4).

32. Chen M, Sandoval H, Wang J. Selective mitochondrial autophagy during erythroid maturation. *Autophagy*. 2008;4(7):926-928.

33. Novak I, Kirkin V, McEwan DG, et al. Nix is a selective autophagy receptor for mitochondrial clearance. *EMBO Rep*. 2010;11(1):45-51.

34. Zhang J, Randall MS, Loyd MR, et al. Mitochondrial clearance is regulated by Atg7-dependent and -independent mechanisms during reticulocyte maturation. *Blood*. 2009;114(1):157-164.

35. Kundu M, Lindsten T, Yang C-Y, et al. Ulk1 plays a critical role in the autophagic clearance of mitochondria and ribosomes during reticulocyte maturation. *Blood*. 2008;112(4):1493-1502.

36. Schweers RL, Zhang J, Randall MS, et al. NIX is required for programmed mitochondrial clearance during reticulocyte maturation. *Proc Natl Acad Sci USA*. 2007;104(49):19500-19505.

37. Diwan A, Koesters AG, Odley AM, et al. Unrestrained erythroblast development in Nix-/- mice reveals a mechanism for apoptotic modulation of erythropoiesis. *Proc Natl Acad Sci USA*. 2007;104(16):6794-6799.

38. Aerbajinai W, Giattina M, Lee YT, Raffeld M, Miller JL. The proapoptotic factor Nix is coexpressed with Bcl-xL during terminal erythroid differentiation. *Blood*. 2003;102(2):712-717.

39. Lee HR, Yoo N, Jeong J, Sohn KY, Yoon SY, Kim JW. PLAG alleviates chemotherapy-induced thrombocytopenia via promotion of megakaryocyte/ erythrocyte progenitor differentiation in mice. *Thromb Res*. 2018;161:84-90.

40. Shen B, Zhao X, O'Brien KA, et al. A directional switch of integrin signalling and a new anti-thrombotic strategy. *Nature*. 2013;503(7474):131-135.

41. Sprangers B, Van Wijmeersch B, Luyckx A, et al. Allogeneic bone marrow transplantation and donor lymphocyte infusion in a mouse model of irradiation-induced myelodysplastic/myeloproliferation syndrome (MD/MPS): evidence for a graft-versus-MD/MPS effect. *Leukemia*. 2009;23(2):340-349.

42. Fan X, Wang C, Shi P, et al. Platelet MEKK3 regulates arterial thrombosis and myocardial infarct expansion in mice. *Blood Adv*. 2018;2(12):1439-1448.

43. Ma Q, Zhu C, Zhang W, et al. Mitochondrial PIP3-binding protein FUNDC2 supports platelet survival via AKT signaling pathway. *Cell Death Differ*. 2019; 26(2):321-331.

44. Schmidt RL, Mock DM, Franco RS, et al. Antibodies to biotinylated red blood cells in adults and infants: improved detection, partial characterization, and dependence on red blood cell-biotin dose. *Transfusion*. 2017;57(6):1488-1496.

45. Hoya K, Guterman LR, Miskolczi L, Hopkins LN. A novel intravascular drug delivery method using endothelial biotinylation and avidin-biotin binding. *Drug Deliv*. 2001;8(4):215-222.

46. Jayakumar R, Kusiak JW, Chrest FJ, et al. Red cell perturbations by amyloid beta-protein. *Biochim Biophys Acta*. 2003;1622(1):20-28.

47. Klickstein LB, Barbashov SF, Liu T, Jack RM, Nicholson-Weller A. Complement receptor type 1 (CR1, CD35) is a receptor for C1q. *Immunity*. 1997; 7(3):345-355.